Eur Phys J C **33**, s01, s430–s432 (2004)
Digital Object Identifier (DOI) 10.1140/epjcd/s2004-03-1740-y

EPJ C direct
electronic only

Studies of W + jets production with the CDF detector

Soushi Tsuno, representing the CDF Collaboration

Institute of Physics, University of Tsukuba, Tsukuba, Ibaraki, Japan, e-mail: tsuno@fnal.gov

Received: 7 January 2004 / Accepted: 20 January 2004 /
Published Online: 3 March 2004 – © Springer-Verlag / Società Italiana di Fisica 2004

Abstract. We have studied the W + ≥ n jets process in Tevatron Run II experiment. This is the first result for the CDF Run II experiment. The data used correspond to a total integrated luminosity of 72 pb^{-1} taken from March 2002 through January 2003. The lowest order QCD predictions have been tested with a new prescription of the parton-jet matching, which allows to avoid a theoretical ambiguity of the collinear/infrared enhancement in calculation. We found a good agreement between data and theory in the typical kinematic distributions. The number of events for each inclusive samples up to 3 jets are also compared with Monte Carlo calculations.

PACS. 13.87.Ce Jets Production in large-Q^2 scattering

1 Introduction

In this study, we present a comparison with data and theory on W + jet production in 1.96 TeV $p\bar{p}$ collisions. The fixed cone jet algorithm is used to identify a jet. To avoid a theoretical ambiguity of the collinear/infrared enhancement at the lowest order calculation, we apply a parton-jet matching procedure by requiring the clear definition of the parton separation, where each parton distributes within the particular cone size of a jet with an assumption that the doubly counted phase space will happen presumably in the colinear region, as well as the merging/splitting procedure of the cone jet algorithm. This is the first result for the CDF Run II experiment.

2 Data set

The CDF is successfully taking the collision data since 2002. The data used in this analysis correspond to a total integrated luminosity of 72.0 pb^{-1} taken from March 2002 through January 2003. High-p_T electron triggered samples are used. After good identification cuts on an isolated high-p_T electron and a requirement of an imbalance of calorimeter energy due to the undetected neutrino (missing E_T), a fixed cone jet algorithm, JetClu algorithm [1], is used to define jets. The transverse energy and pseudorapidity (η) coverage of jets are required as

$$E_T \geq 15\,GeV \qquad , \qquad |\eta| \leq 2.4\,. \tag{1}$$

The clustering cone size is 0.4. The merging/splitting criteria is followed by the jet separation method [2] which requires the iterative separation cone between two jets with 95% separation probability estimated by the two partons at the lowest order calculation. We collect the jets samples inclusively, that is, group the $W + \geq$ n jets event samples, where, for instance, an event which has 2 jets is a member of the $W + \geq 2$ jets event sample but at the same time it can be a member of the $W + \geq 1$ jets event sample.

3 Comparisons of theory to data

3.1 Jet E_T distribution

The jet transverse energy E_T distribution is presented in Fig. 1 for each jet process. From the upper-most side, the distributions are the highest E_T in $W + \geq 1$ jets events, the second highest E_T in W + ≥ 2 jet events, and so forth. The data points are presented as a circle dot. The statistical error is only included in this data point. The shade band among the data point is estimated by the fluctuation of the 10% jet energy scale uncertainty. The solid and dashed lines are the LO QCD predictions, except in $W \geq$ 4 jets events, produced by GR@PPA [3] event generator with the energy scale of the squared mass of a W boson (M_W^2 (GeV^2)) and the square of the average value of the parton p_T ($\langle\, p_T\,\rangle^2$ (GeV^2)), respectively, where the renormalization and factorization scales are equivalent denoted as the energy scale. The LO QCD prediction in $W \geq 4$ jets events is produced by the Alpgen [4] event generator with the energy scale of $M_W^2 + p_{TW}^2$. The CTEQ6 averaging over 40 set of PDF is used in the calculation. Those Matrix Element-based event generators are embedded into HERWIG [5] showering Monte Carlo simulation, and then the generated events pass through the full detector simulation. The MC predictions are normalized by the total number of events in each $W + \geq$ n jets data sample.

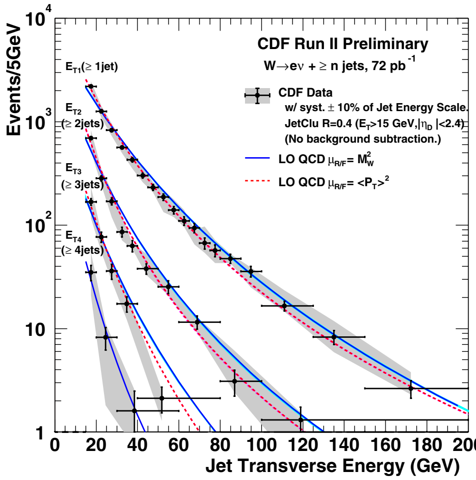

Fig. 1. Jet transverse energy. From the up-most side, the distributions are the highest E_T in $W + \geq 1$ jets events, the second highest E_T in $W + \geq 2$ jets events, and so forth

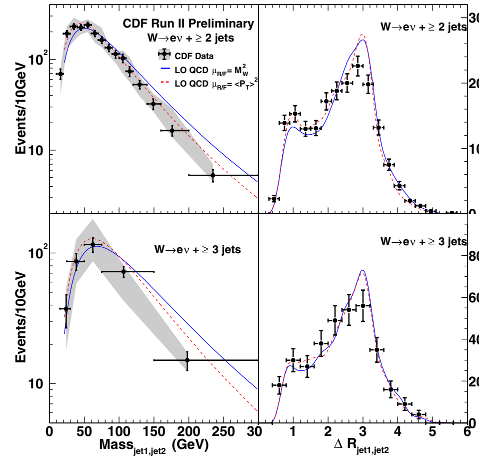

Fig. 2. Dijet mass distribution and jet separation angle between the highest E_T jet and the second highest E_T jet in $W + \geq 2$ jets events and $W + \geq 3$ jets events, respectively

For the MC prediction, the energy scale of $\langle\ p_T\ \rangle^2$ varies with the parton p_T's event by event. The lower energy scale is enhanced by the larger strong coupling α_s since the size of the strong coupling constant increases with the lower energy scale. The shape of the jet E_T distribution thus depends on an order of magnitude of the α_s by event basis. Hence, we can expect that the jet E_T distribution has a sensitivity to the choice of the energy scale. We can see the steeper E_T distribution in the case of $\langle\ p_T\ \rangle^2$ than that of M_W^2. The choice of the energy scale M_W^2 is useful as a good bench mark point to compare not only to the different energy scale but also to the higher order calculation because the running strong coupling constant (scale running) is less meaningful in the NLO calculation. Both MC predictions show a good agreement with the data. The choice of $\langle\ p_T\ \rangle^2$ seems better to describe the data well, but is not clear due to the large jet energy uncertainty.

3.2 Angular and mass distributions

The invariant mass and angular distribution (ΔR_{jj}) between two jets is a sensitive variable to the collinear/infrared singularity. Some differences may be an indicator to the higher order perturbative calculation. In Fig. 2, we present the dijet mass distribution and angular distribution between the highest E_T jet and the second highest E_T jet in the $W + \geq 2$ jets events and the $W + \geq 3$ jets events, respectively.

A discrepancy in both mass distributions of $W + \geq 2$ jets and 3 jets events in the data and MC predictions can be seen in this plot. The mass distributions of MC predictions are harder than those of the data. The distribution is better reproduced by the energy scale of $\langle\ p_T\ \rangle^2$. On the other hand, the ΔR_{jj} distributions are insensitive to the energy scale. These features could be seen in Run I measurement [6]. We see that the theory predictions for the ΔR_{jj} distribution remain valid to the resolution limit of jet-jet separation for our analysis.

3.3 Jet multiplicity

Using the cross section of the MC, we can compare the number of jets distribution with the data. We present the jet multiplicity distribution in Fig. 3. The errors on the data points are the sum of the statistical and systematic uncertainty by the jet E_T scale. The lower and upper band on the LO QCD predictions correspond to the energy scale of M_W^2 and $\langle\ p_T\ \rangle^2$, respectively. On this plot, we did not consider any background contributions. However, those background contaminations are almost negligible in the W + 0,1,2,3 jets events. Indeed, those fractions are ∼2.8%, ∼4.4%, ∼4.7%, and ∼10.1% in the W + 0,1,2,3 jets events, respectively.

The ambiguity for the unphysical parameter like the kinematical cuts on the generator level has been already rejected by the requirement of the parton-jet matching. Since there is only one parton from the MC calculation in the jet cone, the number of jets is proportional to the number of partons, that is, an order of the strong coupling constant. We can see almost linear relation of the jet multiplicity in both the data and MC's. This shows our analysis method well describes the enhance lowest order phase space. The difference of the absolute cross section will be addressed as a lack of the higher order calculations.

3.4 Ratio of the jet multiplicity

We show various ratio plots to each jet bin in $W + \geq$ n jets events in Fig. 4. From the top, the ratio of theory to data, the ratio of n jets events to n-1 jets events, and the ratio to the ratio of n jets events to n-1 jets events,

$$R_{n/(n-1)} = \frac{\sigma_n}{\sigma_{n-1}}\ , \tag{2}$$

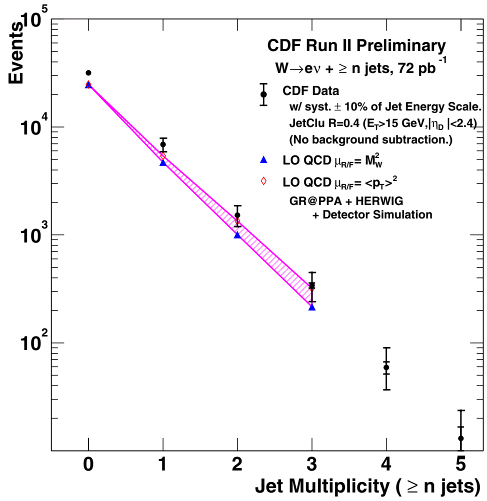

Fig. 3. Jet multiplicity distribution. The errors on the data points are the sum of the statistical and systematic uncertainty by the jet E_T scale. The lower and upper band on the LO QCD predictions correspond to the energy scale of M_W^2 and $\langle\, p_T \,\rangle^2$, respectively

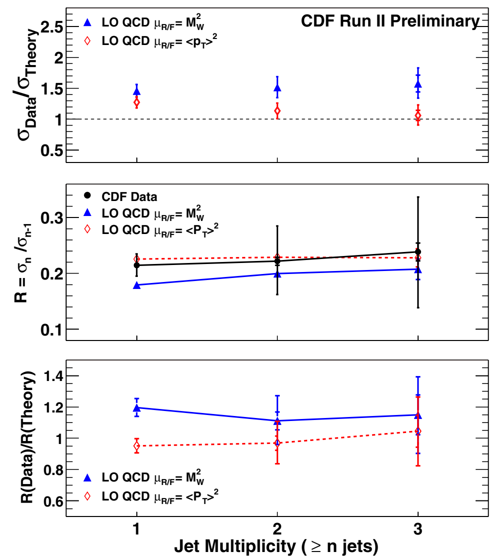

Fig. 4. Ratio of jet multiplicity. From the *top*, the ratio of theory to data, the ratio of n jets events to n-1 jets events, and the ratio to the ratio of n jets events to n-1 jets events are shown

are presented. Taking the ratio of the physics variable is to cancel out the uncertainties from the absolute source like the luminosity. The identification efficiency or acceptance etc. may also cancel somehow out.

We see that the absolute cross section predictions agree with the data within a factor of less than 2. Those factors are ∼1.2 for the energy scale of $\langle\, p_T \,\rangle^2$ and ∼1.5 for M_W^2 over the range to the $W + \geq 3$ jets events, respectively. Remarkable feature is that the MC predictions show almost constant behavior in this ratio plot. That means that our analysis method and MC prediction well describe the data. It is interesting to see the ratio $R_{n/(n-1)}$ (middle). The jet counting uncertainties are reduced except for $R_{1/0}$. The $R_{n/(n-1)}$ comparison is valid if higher order QCD corrections to the LO cross sections are not strongly dependent on the number of final state partons. The ratio $R_{n/(n-1)}$ measures the decrease in cross section with the addition of 1 jet. The value of $R_{n/(n-1)}$ thus is clearly dictated by the magnitude of the strong coupling constant since adding an extra jet adds a factor of α_s. We can see the energy scale $\langle\, p_T \,\rangle^2$ gives a better agreement than the M_W^2. In the $R_{n/(n-1)}$ plot, the particular value of $R_{n/(n-1)}$ will vary as a function of the specific jet E_T requirement that define a jet. To remove this dependence to some degree, the ratio (bottom) of data and theory for $R_{n/(n-1)}$ give a sensitivity to an independent comparison of the jet definition and its systematics. With accurate theory predictions and accurate data measurements the value of this ratio is 1.0. If the QCD predictions reproduce the jet kinamtics accurately, the ratio of data to theory is independent of the choice of the jet E_T requirement so that the quantity may be of more general interest.

4 Conclusion

Data have been compared to the theory predictions at the lowest order perturbative calculation level. Jet separation procedure based on the parton-jet matching requirement is used for the data and theoretical predictions. This requirement is to avoid a theoretical ambiguity of the collinear/infrared enhancement in calculation. For the theory prediction, two choices of the energy scale, $\langle\, p_T \,\rangle^2$ and M_W^2, where the renormalization and factorization scales are equivalent, has been tested. The jet transverse energy, mass and jet-jet separation distribution were compared between data and theory predictions, and showed good agreements. The choice of the energy scale of $\langle\, p_T \,\rangle^2$ is preferred to describe data well. Jet multiplicity distribution was also compared up to $W + \geq 3$ jets events. The constant (flat) behavior can be seen in the various ratio plots. This is very important feature to certify our rightness of the MC generation and analysis scheme, which is crucial for the measurement of the strong coupling constant. We'd also like to mention that the NLO event generator is a key point for this study.

References

1. F. Abe et al.: Phys. Rev. Lett. **74**, 2626 (1995)
2. S. Tsuno: in preparation
3. S. Tsuno et al.: Comput. Phys. Commun. **151**, 216 (2003)
4. M.L. Mangano et al.: J. High Energy Phys. **07**, 001 (2003)
5. G. Marchesini and B.R. Webber, Nucl. Phys. B **310**, 461 (1988);
   G. Marchesini et al.: Comput. Phys. Commun. **67**, 465 (1992)
6. T. Affolder et al.: Phys. Rev. D **63**, 072003 (2001)